ELSEVIER

Journal of Membrane Science 176 (2000) 177–196

journal of MEMBRANE SCIENCE

www.elsevier.nl/locate/memsci

Multi-objective optimization of membrane separation modules using genetic algorithm

Chan Ching Yuen, Aatmeeyata, Santosh K. Gupta[1], Ajay K. Ray*

Department of Chemical and Environmental Engineering, National University of Singapore, 10 Kent Ridge Crescent, Singapore 119260, Singapore

Received 16 September 1999; accepted 10 April 2000

Abstract

Hollow fiber membrane separation modules are used extensively in industry for a variety of separation processes. In most cases, conflicting requirements and constraints govern the optimal choice of decision (or design) variables. In fact, these optimization problems may involve several objectives, some of which must be maximized, while the others minimized *simultaneously*. Often, a set of equally good (non-dominated or Pareto optimal) solutions exist. In this study, a membrane separation module for the dialysis of beer has been taken as an *example* system to illustrate the multi-objective optimization of *any* membrane module. A mathematical model is first developed and 'tuned' using some experimental results available in the literature. The model is then used to study a few simple multi-objective optimization problems using the non-dominated sorting genetic algorithm (NSGA). Two objective functions are used: the alcohol removal (%) from the beer is maximized, while simultaneously minimizing the removal of the 'extract' (taste chemicals). Pareto optimal solutions are obtained for this module. It was found that the inner radius of the hollow fiber is the most important decision variable for most cases. Another optimization problem using the cost as the third objective function is also solved, using a combination of the ε-constraint method and NSGA. It is found that the Pareto solutions lie on a *curve* in the three-dimensional objective function space, and do not form a *surface*.

Keywords: Membrane separation module; Genetic algorithm; Pareto sets; Optimization problem; Beer dialysis

1. Introduction

Membrane separations have become quite popular in chemical engineering in the last 30 years [1]. Large-scale commercial uses of membrane separation processes have displaced conventional separation processes in several areas, as they are more capital and energy efficient when compared with distillation, absorption and adsorption, etc. The rapid development of membrane technology can be attributed to significant breakthroughs in the development of membranes, membrane modules and equipment design. Modern membranes couple high transmembrane fluxes with high selectivity. The development of hollow fiber and spiral wound designs improves the efficiency of these processes while new equipment designs can now successfully handle concentration polarization and other problems commonly encountered.

The design of membrane separation modules is associated with several important objectives, which

* Corresponding author. Tel.: +65-874-8049; fax: +65-779-1936.
E-mail address: cheakr@nus.edu.sg (A.K. Ray)
[1] Present address: Department of Chemical Engineering, University of Wisconsin, Madison, WI 53706, USA. On leave from Indian Institute of Technology, Kanpur 208016, India.

0376-7388/00/$ – see front matter
PII: S0376-7388(00)00440-3

need to be optimized, as well as many constraints. Rigorous optimal designs of membrane modules would help in further increasing their competitiveness. Unfortunately, not much work has been reported in the open literature on the multi-objective optimization of membrane separation systems. To the best of our knowledge, this is the first attempt at addressing such a problem. In this paper, we select one simple representative *example* from among a whole variety of membrane separation systems, namely, the optimization of beer dialysis modules. The method of optimization used in this work is very general, and can easily be applied to almost any other membrane separation module, e.g. those used for desalination, etc. In fact, in this paper, we *illustrate the procedure* to be used, and present solutions of a few relatively *simple* optimization problems with two objective functions and a few constraints. A whole variety of other problems can, indeed, be formulated and solved, depending upon one's interest. We hope this paper will spur research in this important area.

In the last few years, considerable emphasis has been put on the use of membrane separation modules for processes involving the production of beers with reduced alcohol content. It is obvious that diets, increasing health consciousness, food regulations and traffic laws of many countries have led to this interest. It is this process which we consider for optimization in the present study. Until recently, there were two main ways to manufacture beer having low alcohol content [2,3]. The first is to influence the fermentation process itself by using special yeast, special fermentation behavior, disruption of the fermentation process, etc. This has been a very economical way. Unfortunately, beers produced by this method lack either the full body due to too little original wort, or have an atypical flavor due to incomplete fermentation. This has led to the development of expensive post-fermentation processes, such as dilution, distillation and reverse osmosis. Beers made from these processes are also not satisfactory in regard to their organoleptic properties.

A new process that makes it possible to lower the alcohol content of regular beer without falsifying its 'character' involves the use of dialysis [2]. Dialysis is a rate-governed membrane process in which a solute in the feed solution is driven across a semi-permeable membrane by means of a concentration gradient. In beer dialysis, all the beer ingredients (alcohol as well as the higher molecular weight compounds giving beer its characteristic taste) will try to diffuse. The rate of diffusion is directly proportional to the concentration gradient and inversely proportional to the molecular size. As an initial approximation, two solutes can be separated by dialysis if their diffusion coefficients in the feed differ by at least an order of magnitude [1]. It is clear that the alcohol (ethanol) diffuses preferentially through the membrane, as compared to the taste chemicals (referred to as extract). The most important requirement of beer dialysis is that the taste and full-body of the feed beer is retained as much as possible, while maximizing the dialysis of alcohol. Thus, beer dialysis provides an excellent example for multi-objective optimization studies, and indeed, it is being used to provide the example in this study.

Hollow fiber modules have established themselves as an excellent choice for beer dialysis. Some experimental research has been reported in this area. A dialysis unit processing $1.5\,m^3/h$ of beer, whose alcohol content was to be reduced by about 40%, was experimentally demonstrated by Moonen and Niefind [2]. Also, Leskosek et al. [3–5] have published some experimental results on a laboratory-scale hollow fiber beer dialysis module which could help in the development of a simple model for this operation.

In this work, a mathematical model is first developed for the beer dialysis module. The experimental results of Leskosek et al. [3–5] are used to provide estimates of a few variables and parameters required in the model. Thereafter, multi-objective Pareto optimal solutions are generated for use in the design and operation of a beer dialysis module using genetic algorithm (GA). GA is a non-traditional search and optimization method [6–9], that has become quite popular in engineering optimization. It mimics the principles of genetics and the Darwinian principle of natural selection (i.e. survival of the fittest). Simple genetic algorithm (SGA) is suitable for optimizing problems with a single objective function. In single objective function optimization, one attempts to find the best design, which is usually the global minimum (or maximum). Most real world problems involve the simultaneous optimization of multiple objective functions (a vector). Such problems are conceptually different from single objective function problems. In multiple objective function optimization, there may not exist a solution that is the best (global optimum)

with respect to all objectives. Instead, there could exist an entire set of optimal solutions that are *equally* good. These solutions are known as Pareto-optimal (or non-dominated) solutions. A Pareto set, for example, for a two-objective function problem is described by a set of points such that when one moves from one point to any other, one objective function improves, while the other worsens. Thus, one cannot say that any one of these points is superior (or dominant) to any other. Since none of the non-dominated solutions in the Pareto set is superior to any other, any one of them is an acceptable solution. The choice of one solution over the other requires additional knowledge of the problem, and often, this knowledge is intuitive and non-quantifiable. The Pareto set, however, is extremely useful since it narrows down the choices and helps to guide a decision-maker in selecting a desired operating point (called the preferred solution) from among the (restricted) set of Pareto-optimal points, rather than from a much larger number of possibilities.

In earlier years, multi-objective optimization problems were usually solved using a single *scalar* objective function, which was a weighted-average of the several objectives ('scalarization' of the vector objective function). This process allows a simpler algorithm to be used, but unfortunately, the solution obtained depends largely on the values assigned to the weighting factors used, which is done quite arbitrarily. An even more important disadvantage of the scalarization of the several objectives is that the algorithm may miss some optimal solutions, which can never be found, regardless of the weighting factors chosen. This happens if the non-convexity of the objective function gives rise to a duality gap [9–11]. Several methods are available to solve multi-objective optimization problems, e.g. the ε-constraint method [12–14], goal attainment method [10,15,16] and the non-dominated sorting genetic algorithm (NSGA) [7,9,17,18]. In this study, we use NSGA to obtain the Pareto set. This technique offers several advantages [9], as for example:

1. its efficiency is relatively insensitive to the shape of the Pareto optimal front;
2. problems with uncertainties, stochasticities, and with discrete search spaces can be handled efficiently;
3. the 'spread' of the Pareto set obtained is excellent (in contrast, the efficiency of other optimization methods decides the spread of the solutions obtained);
4. it involves a single application to obtain the entire Pareto set (in contrast to other methods, e.g. the ε-constraint method, which needs to be applied several times over).

Indeed, NSGA has been applied recently to optimize several processes of industrial importance in chemical engineering, including an industrial nylon-6 semi-batch reactor [18,19], a wiped-film polyester reactor [20], a steam reformer [21] and cyclone separators [22]. These form the subject of a recent review [23].

2. Modeling of the beer dialysis module

As mentioned earlier, hollow fiber membrane modules are used in the production of low alcohol beer. The beer (feed) flows through the hollow fibers while water (dialysate) flows in the opposite direction on the outside of the Cuprophan (from cellulose) fibers [2–5]. This countercurrent flow arrangement achieves a favorable concentration gradient along the entire membrane and is very efficient. The assumptions made in the model are as follows: (i) there is ideal countercurrent flow in the membrane module for efficient mass transfer; (ii) steady state exists on both the shell and tube sides of the membrane; (iii) transmembrane pressure is negligible. This is typical of dialysis with liquid phases on both sides of the membrane. However, it was reported [3–5] that due to its complex, one or two phase colloidal nature, beer does not behave as a normal liquid–liquid dialysis system and a small pressure is needed on the beer side to avoid the osmotic flux of water and beer dilution. Based on this, it is further assumed that water does not diffuse across the membrane; (iv) the presence and effect of any dissolved gas (e.g. CO_2) normally used in beer dialysis [2] to contribute to better overall taste of the beer is neglected; (v) the hollow fibers in the tube are arranged in a triangular pitch; (vi) a constant temperature is maintained; (vii) the physical properties, such as density and viscosity, of the fluids are assumed to be constant and (viii) a single hollow fiber membrane module is used in the process. The model equations are easy to write [24–26] and the complete set of equations is given in Appendix A. It is observed from these equations that

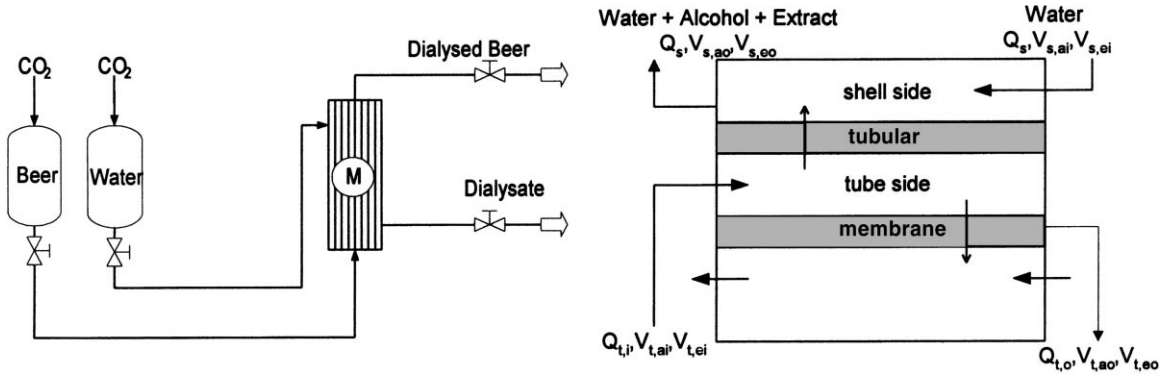

Fig. 1. Laboratory system for beer dialysis and a schematic of a membrane module used in beer dialysis.

we need to solve a system of five non-linear equations involving the following five dependent variables: $Q_{t,o}$, $V_{s,ao}$, $V_{t,ao}$, $V_{s,eo}$ and $V_{t,eo}$ (see Section 5 and Fig. 1). These variables, representing the output flow rates and concentrations of each of the two components (alcohol, a and extract, e), can be solved using a non-linear algebraic equation solver for any given module, for a specified set of operating conditions.

Before we solve any optimization problem, it is a common practice to make sure that the model is good. In addition, experimental data is required to evaluate values of the parameters in the model, which are difficult to estimate on an a priori basis. We also need to decide the values of some of the 'input' variables (operating conditions and parameters) characterizing the unit to be optimized. For example, we need to fix values of variables like the flow rate of the feed to be processed, the composition of the feed, etc., which describe the unit whose performance we wish to optimize. For these, we select (for illustration purposes, again) the lab-scale beer dialysis module of Leskosek et al. [4]. We use the (scarce) experimental data [4], on the percent removal of alcohol and extract (taste chemicals) at different flow rates of the beer in this module. Fig. 2 shows this data, and Table 1 gives the details of the module and the operating conditions used. The concentrations of alcohol and extract in the exit streams have been obtained according to the methods recommended in brewing practice [3–5]. Unfortunately, Leskosek et al. did not provide values of two variables describing their experimental module, namely, the length, l, of the individual hollow fibers, and φ, the fractional free area in the shell. In addition, our model requires the value of the parameter, P_{ma}, the diffusive permeability of alcohol in the membrane. We decided to assume [1] that l=0.8 m, and to use φ and P_{ma} as parameters whose values are to be obtained by 'tuning' against the experimental data shown in Fig. 2. It may be mentioned that if values of l and φ were available to us for the experimental module, we would have had to tune only one parameter, P_{ma}. The assumption, that l=0.8 m is not too critical, since the total membrane area is known, and the mass transfer coefficient does not change much with changing length. Indeed, we found that model predictions of the alcohol and extract removal did not vary much with the length (for identical input conditions and total membrane area).

An additional assumption was made in our study to keep the model simple. The extract comprises of a whole range of different chemical compounds, involving molecules having relatively large molecular weights, ranging from 10^2 to 10^5 Da [5]. These molecules are primarily saccharides, dextrins, and other 'taste chemicals' that contribute to the color, bitterness and pH of beer. Modeling the diffusion of so many molecular species through the membrane would be almost impossible and meaningless, particularly since experimental data is not available for the removal of each of these species so as to estimate their permeabilities. We assume, therefore, that the diffusion of these several species in the extract can be described satisfactorily by the diffusion of a single *pseudo*-species, namely, an oligo-saccharide, (i.e. a straight-chain molecule comprising of (z+2) glucose units (see Fig. 3)) having z=8 and with a molecular

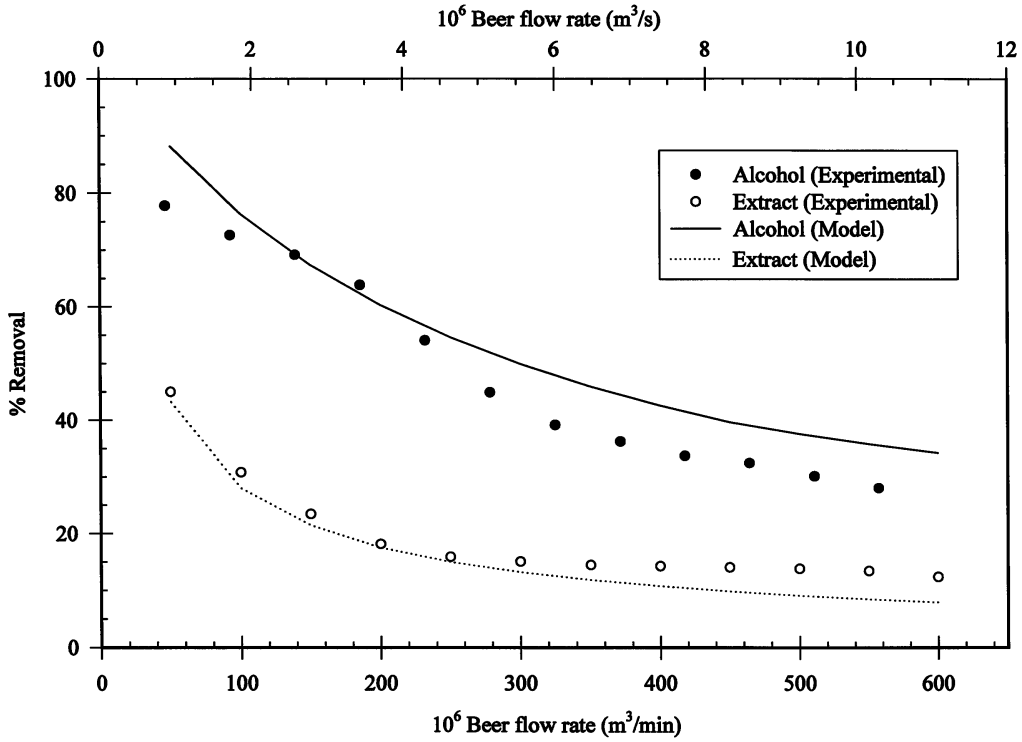

Fig. 2. A comparison showing the removal of alcohol and extract predicted by our model (curves) and experimental data (symbols) after convergence (tuning). Feed flow rates of water (shell side) and beer (tube side) are the same. Equally spaced points are taken from the curves published in [4].

Table 1
Equipment and operating parameters for the experiment by Leskosek et al. [4]

Equipment/operating parameters	Values [4]
Membrane material	Cuprophan (regenerated cellulose)
Membrane type	Hollow fiber
Total membrane area, A_T (m^2)	1.3
Membrane thickness, t (μm)	8
Internal radius of each hollow fiber, r_i (μm)	100
Alcohol content of beer in feed (% (w/w))	3.8 ($V_{t,ai}$=0.0471)
Extract content of beer in feed (% (w/w))	12 ($V_{t,ei}$=0.08)
Operating temperature (K)	278
Operating pressure (both tube and shell sides) (kPa)	100 (absolute)
Transmembrane pressure	0
Flow rate of beer (tube)[a], $Q_{t,i}$(m^3/s)	8.33×10^{-7}–1.0×10^{-5}
Flow rate of water (shell)[a], Q_s (m^3/s)	8.33×10^{-7}–1.0×10^{-5}
Beer/water feed flow ratio (v/v)	1:1
Length of each fiber, l (m)	0.8 (assumed)
Fractional free area, φ	0.727 (tuned value)
Flow arrangement — countercurrent	Beer in the hollow fibers and water in the shell
Alcohol content in feed water	0
Extract content in feed water	0

[a] Values used for optimization (Eqs. (2a) and (2b)): $Q_{t,i}=4.17\times10^{-6}$ m^3/s; Q_s obtained by optimization.

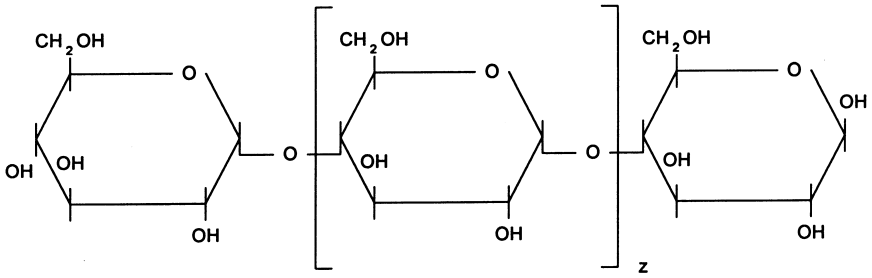

Fig. 3. An oligosaccharide molecule.

weight of 1314. We did try to use z as an additional tuning parameter (rather than fixing it at 8) but this did not lead to any better agreement of model predictions with experimental data (see discussion later). The assumed value of z is not too high since it lies inside the range suggested by Leskosek et al. [5]. Also, the overall rate of diffusion of the pseudo-species represents the complex diffusion of the multi-component system, which is a highly non-linear function of the molecular weights and concentrations of the several species present (and we should not attempt to assign any physical meaning to this value of z).

A function, F_{val}, which was taken to be the sum of squares of the differences between the values given in Fig. 2 and those predicted by our model, was defined as follows:

$$F_{\text{val}} = \sum_{8.33\times10^{-7}\,\text{m}^3/\text{s}}^{1.0\times10^{-5}\,\text{m}^3/\text{s}} \left\{ \left[\frac{R_{\text{a,model}} - R_{\text{a,expt}}}{R_{\text{a,model}}} \right]^2 + \left[\frac{R_{\text{e,model}} - R_{\text{e,expt}}}{R_{\text{e,model}}} \right]^2 \right\} \quad (1)$$

where R_{a} and R_{e} are the percentage removals for alcohol and extract, respectively. The sum of squares was normalized with respect to the percentage removals predicted by the model. The terms in Eq. (1) are calculated for each of the experimental data points (since only continuous curves were available in [4], we took equi-spaced 'experimental' data points at intervals of $8.33\times10^{-7}\,\text{m}^3/\text{s}$, in the range of beer flow rate from 8.33×10^{-7} to $1.0\times10^{-5}\,\text{m}^3/\text{s}$ (50×10^{-6}–$600\times10^{-6}\,\text{m}^3/\text{min}$). F_{val} was minimized using a direct search complex algorithm, which performs a non-linear least squares curve-fit. F_{val} represents an overall deviation of the model predictions from the experimental results in Fig. 2.

For each run, a value for each of the two tuning variables, φ and P_{ma}, is selected lying within user-supplied bounds. These values are used in the model equations with the physical properties and parameters given in Table 2. These equations are, in turn, solved by the non-linear equation solver. The solver returns values of R_{a} and R_{e}, which are used to evaluate F_{val} for any selected set of values of φ and P_{ma}. Ultimately, a minimum value of F_{val} was found for $\varphi=0.727$ and $P_{\text{ma}}=3.279\times10^{-5}\,\text{m/s}$. A comparison between model predictions (solid lines) and experimental data (symbols) for these tuned values of φ and P_{ma}, is shown in Fig. 2. The figure shows that the tuned model is able to predict values for the percentage removal of alcohol and extract, which are quite close to the published experimental results in the literature [4]. Furthermore, it was reported that the permeability

Table 2
Physical properties and parameters used

Parameter	Value	Source/remarks
μ_{w} (Pa s)	0.0015	[24]
ρ_{w} (kg/m^3)	1000	[24]
ρ_{a} (kg/m^3)	806	[24]
ρ_{e} (kg/m^3)	1500	Pure mono- and di-saccharides [24]
M_{a}	46	Pure ethanol [24]
M_{e}	1314	z=8 in Fig. 3
D_{aw} (m^2/s)	8.10×10^{-10}	Appendix A (Eq. (A.7))
D_{ew} (m^2/s)	1.33×10^{-10}	Appendix A (Eq. (A.8))
P_{ma} (m^2/s)	3.28×10^{-5}	Tuned value
P_{me} (m^2/s)	1.36×10^{-6}	Appendix A (Eq. (A.10))
ψ_{w}	2.6	[25]
v_{a}	59.2	Ethanol [25]

of a typical Cuprophan membrane for molecules of ethanol may be assumed to be about 25 times higher than for an oligo-saccharide with an average molecular weight of about 2000 [5]. In the tuning done here, a calculation shows that the difference in permeability is about 24 times. This is sufficiently close.

The value of the fractional free area in the shell, φ, obtained by the tuning of (the very small amount of) experimental data taken on the *lab-scale* module of Leskosek et al. [4], appears to be high when compared to actual values for *commercial* modules, which range from about 0.37 to 0.5 [1]. This discrepancy indicates that the model needs refinement before *physically* meaningful values of the parameters are obtained. Extensive experimental results also need to be generated to test future detailed models and evaluate their parameters. Pressure drop data on both the inside and outside of the hollow fibers, are also needed for testing of improved models. However, it must be emphasized that Fig. 2 does, indeed, give reasonably good agreement between experimental results and model predictions, and so we could expect that results from our optimization study would still be meaningful, even with the present, purely 'curve-fitted' value of φ.

An attempt was also made to tune the experimental data using three tuning variables/parameters, namely, φ, P_{ma} and z, the number of glucose rings in the extract molecule. When doing this, provision was made to ensure that z is always an integer. However, the tuned value of z came out to be 2 (which is too low for a typical extract molecule), with φ not being much lower than before, and so we decided to use z=8 and the previous value of φ=0.727 for the optimization. It must be mentioned that even though it would have been far more satisfying if we had obtained physically meaningful values for all the tuned parameters, *simple* models of complex processes need not necessarily satisfy this expectation always, particularly when the amount of experimental data is extremely small. Attempts to improve models continue, even while models describing available experimental data satisfactorily are used for optimization.

3. Multi-objective optimization of beer dialysis

Non-dominated sorting genetic algorithm was used with the tuned model described above to optimize the beer dialysis module. It is to be emphasized again that there is no end to the variety of multi-objective optimization problems, which could be formulated and studied, and we present a few simple examples here, to illustrate the concepts, techniques, and interpretation of results. Multi-objective Pareto optimal solutions are generated here for use in both the operating and design phases of beer dialysis. In order to ensure that physically meaningful results are obtained, constraints on pressure drops on both the shell and tube sides in the module were added to our model. These constraints are necessary to ensure that the pressure drops stay within reasonable limits.

3.1. Multi-objective optimization of the operation of an existing module

The *operation* of the lab-scale module [4] (used for tuning our model) is first optimized. Only a single decision variable, Q_s (the inlet flow rate of pure water), is used. We choose two objective functions — minimization of R_e, the percent removal of the extract chemicals, and the maximization of R_a, the percent removal of alcohol from the beer. Since the computer code available with us for NSGA minimizes the objective functions, we need to transform the second objective function into one involving minimization. Several candidates are available for this, but probably the simplest and the most popular form (which also does not change the location of the solutions [8]) is to minimize $f_2 \equiv 1/(1+R_a)$, rather than maximize R_a. Thus, the optimization problem studied is represented mathematically by

$$\min f_1(Q_s) = R_e \tag{2a}$$

$$\min f_2(Q_s) = \frac{1}{1+R_a} \tag{2b}$$

such that (s.t.)

$$0 \le \Delta P_t \le 51.7\,\text{kPa}\ (7.5\,\text{psi}) \tag{2c}$$

$$0 \le \Delta P_s \le 10.3\,\text{kPa}\ (1.5\,\text{psi}) \tag{2d}$$

$$d_s = 0.02103\,\text{m} \tag{2e}$$

$$\text{model equations (Appendix A)} \tag{2f}$$

The choice of the two objective functions, f_1 and f_2, in Eqs. (2a) and (2b) enable the production of beer having a low-alcohol content while having a good taste.

Table 3
Computational parameters of NSGA [17] used in this work

Maximum generation, N_{maxgen}	400
Population size, N_{pop}	50
Sub-string length coding for each decision variable, l_i	32
Crossover probability, P_{cross}	0.8
Mutation probability, P_{mute}	0.0001
Maximum niche count distance, σ_{share}	0.001
Exponent in sharing function, α	2.0
Seed for random number generator	0.5

The above equations provide an excellent example of how two objectives which cannot really be compared by putting them together into a single, scalar objective function, can be used as components of a vector objective function.

The physical properties, operating parameters and module dimensions used for this optimization problem are given in Tables 1 and 2. The value of $Q_{t,i}$ is fixed (for illustration) for the optimization study, as 4.17×10^{-6} m^3/s, which lies somewhere midway in Fig. 2. The bounds on the only decision variable used, Q_s, are 5×10^{-6}–10×10^{-6} m^3/s (note that $Q_s \neq Q_t$ for optimization). It is to be noted that the flow rate of beer used for optimization is quite low, and corresponds to one of the values used in the *laboratory* unit by Leskosek et al. [4] In fact, this low flow rate is the reason why d_s in Eq. (2e) is quite small. Table 3 shows the computational parameters used to obtain the solutions. The values presented in Tables 2 and 3 were kept unchanged for all the other optimization runs in this work.

The computer program consisting of the tuned model and NSGA was tested and run on a Silicon Graphics SGI Origin2000 supercomputer. The CPU time was extremely small and allowed us to obtain solutions interactively. The results of this optimization problem are presented in Fig. 4. Fig. 4a shows the Pareto set obtained, while Fig. 4b gives the flow rate of water, Q_s (the only decision variable in this run), corresponding to each of the points on the Pareto. It can easily be confirmed that the points in Fig. 4a do, indeed, constitute a Pareto set, i.e. as the alcohol removal increases (desirable), the extract removal increases (undesirable). For the fixed beer flow rate at the tube inlet, Fig. 4b shows that the water flow rate on the shell side has to be increased to affect

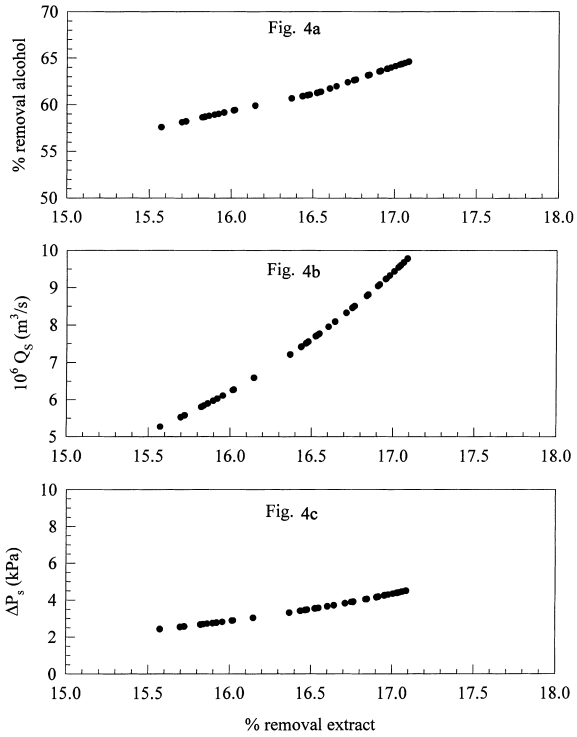

Fig. 4. Pareto set and corresponding values of Q_s and ΔP_s for the optimization of the operation of an existing module.

higher removal of alcohol, but at the cost of higher extract removal. This is expected intuitively. Due to this increase in the flow rate of water (with r_i, t, l and φ fixed), it is obvious that the pressure drop on the shell side will increase. This is reflected in Fig. 4c. For this run, the tube side pressure drop (same for all the Pareto points) is calculated to be 47.1 kPa. A decision-maker working with this membrane module can select an operating point (preferred solution) from among those given in Fig. 4a.

It may be emphasized again that this optimization problem represents just one example of the use of multi-objective optimization and the techniques described herein can be used for any similar optimization of an existing membrane separation module. It may be added that the experimental point of Leskosek et al. [4] with $Q_s = Q_t$ (for a beer flow rate of 4.17×10^{-6} m^3/s), would have been a part of the Pareto set for this problem with one decision variable, if we had selected a larger range for Q_s.

3.2. Optimization of a beer dialysis module at the design level

Optimization at the *design* stage for any problem, including the beer dialysis one, provides far more freedom than when one is constrained to optimize the performance of an *existing* module. At the design stage, several additional decision (or design) variables become available for optimization. A meaningful optimization problem for beer dialysis could be the following (again, this is an example, and several other alternatives are possible):

$$\min f_1(Q_s, r_i, l, \varphi, t) = R_e \quad (3a)$$

$$\min f_2(Q_s, r_i, l, \varphi, t) = \frac{1}{1 + R_a} \quad (3b)$$

s.t.

$$0 \leq \Delta P_t \leq 51.7\,\text{kPa (7.5 psi)} \quad (3c)$$

$$0 \leq \Delta P_s \leq 10.3\,\text{kPa (1.5 psi)} \quad (3d)$$

$$d_s = 0.02103\,\text{m} \quad (3e)$$

model equations (Appendix A) (3f)

The decision variables for this problem are taken as (i) the flow rate of (pure) water on the shell side, Q_s; (ii) the internal radius of a single hollow fiber, r_i; (iii) the length of the fiber, l; (iv) the fractional free area in the shell, φ (related to the tube pitch, P_t) and (v) the thickness of the hollow fiber membrane, t. These choices would usually be available at the design stage. A fixed value of the inner diameter of the shell (using the value for the 'tuned' model as a somewhat arbitrary choice, since the beer feed flow rate is taken to be of the same order of magnitude as for Fig. 2) is assumed again. This is to ensure that every point in the Pareto set corresponds to a module with an identical shell (otherwise, there are far too many degrees of freedom available in the optimization problem). The effect of relaxing this requirement is studied later.

The bounds of the decision variables used are tabulated in Table 4 (Problem no. 1). Results of the multi-objective optimization problem defined in Eqs. (3a)–(3f) are shown in Figs. 5–7. The Pareto optimal set is shown in Fig. 5a, while the five decision variables (Q_s, r_i, l, φ and t) corresponding to the points on the Pareto set are shown in Fig. 5b and c and Fig. 6a–c, respectively. It is found that the optimal values of four of these five decision variables are almost constant (Q_s, φ and t at their upper bounds, l at its lower bound), and only r_i decreases as the values of R_a and R_e increase. As expected, the total membrane area, A_T, influences the Pareto set quite significantly (Fig. 7a). A_T, in turn, can be changed using *any* one or more of the four decision variables (r_i, l, φ, and t) selected in this study. However, it is observed that r_i is the most sensitive variable as changes in the total membrane area are being achieved in this case by changing r_i *alone*, with the other decision variables (l, φ and t) at constant values. It should also be noted that higher values of r_i in Problem no. 1 (Fig. 6a) lead to lower values of the total available membrane area (d_s being fixed). This enables achievement of lower levels of alcohol and extract removals (compared to Fig. 4a where r_i is fixed

Table 4
Description of parameter values used to study Problem nos. 1–13

	Decision variable	Reference	Effect of Q_s		Effect of l		Effect of φ		Effect of t		Effect of ΔP		Effect of d_s
Problem no.	1	2	3	4	5	6	7	8	9	10	11	12	13
10^6 Q_s (m^3/s)	5–10	10	3.33	16.7	10.0		10.0		10.0		5–10		5–10
l (m)	0.5–1.0	0.5	0.5		0.2	0.8	0.5		0.5		0.5–1.0		0.5–1.0
φ	0.65–0.75	0.75	0.75		0.75		0.65	0.85	0.75		0.65–0.75		0.65–0.75
t (μm)	5–25	25	25		25		25		5	45	5–25		5–25
r_i (μm)	For Problem nos. 1–13: r_i=80–300												
A_T (m^2)	Calculated[a]												0.05–0.8
Δp_t (kPa)	For Problem nos. 1–10: $\Delta p_t \leq$51.7 kPa (7.5 psi)										$\leq 5.17\times10^4$	$\leq$5.52	$\leq$51.7
Δp_s (kPa)	For Problem nos. 1–10: $\Delta p_s \leq$10.3 kPa (1.5 psi)										$\leq 1.03\times10^4$	$\leq$3.45	$\leq$10.3
d_s (m)	For Problem nos. 1–12: d_s=0.02103 m												Calculated[a]

[a] No *explicit* constraint (calculated from optimum values of r_i, φ, l and t).

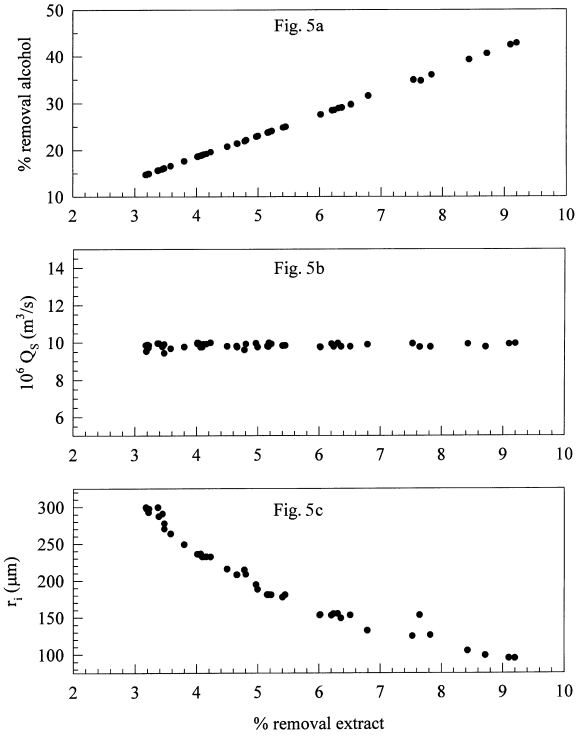

Fig. 5. Pareto set for Problem no. 1 and values of the decision variables (Q_s and r_i) corresponding to the points on the Pareto set in Fig. 5a.

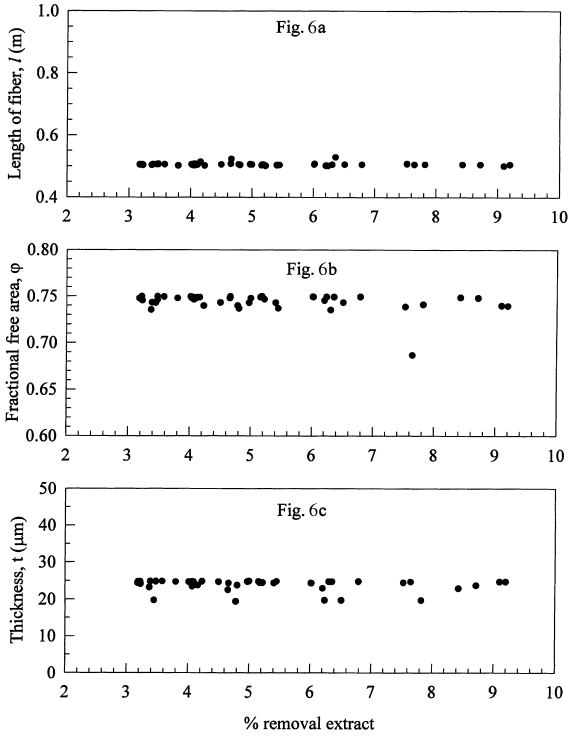

Fig. 6. Values of the decision variables (l, φ and t) corresponding to the points on the Pareto set in Fig. 5a.

at 100 μm), and lower values of the pressure drops on both the shell (Figs. 4c and 7c) and tube sides. It is interesting to observe (Fig. 7b) that the upper bound on ΔP_t of 51.7 kPa controls the choice of the lowest optimal value of r_i.

A comparison of Figs. 4–7 leads to the interesting inference that when Q_s is taken as the *only* decision variable (Eqs. (2a) and (2b)), it varies along the Pareto optimal solutions (Fig. 4b). In contrast, when Q_s is taken as *one of five* decision variables (along with r_i, l, φ, and t), it takes on a constant value. In fact, in the latter case, r_i emerges as the single dominant decision variable, varying along the Pareto optimal points, while all the other four decision variables take on constant values either at their upper or lower bounds. A similar phenomenon of dominating decision variables was observed in our earlier multi-objective optimization study of trains of cyclone separators [22]. This is a manifestation of the sensitivity of the objective functions to the decision variables. For the present study, an approximation analysis can be carried out to explain this effect. The equations in Appendix A lead to the following *approximate* functional relation (for Reynolds numbers below 2100, corresponding to the optimal solutions)

$$\text{Rate of mass transfer (for alcohol, a, and extract, e)} \sim \frac{1}{r_i^{4/3}(C_1 + C_2/Q_s^{1/3})} \quad (4)$$

In this equation, C_1 and C_2 are constants (different for a and e) under the conditions of interest. Eq. (4) suggests that when Q_s is the *only* decision variable, an increase in Q_s leads to an increase in the rates of mass transfer, and so leads to higher values of both R_a and R_e. Our technique picks up this dependence during optimization (Fig. 4a and b). On the other hand, Eq. (4) shows that the rates of mass transfer are far more sensitive to variations in r_i than in Q_s, due to the higher exponent on r_i. A relatively small decrease in

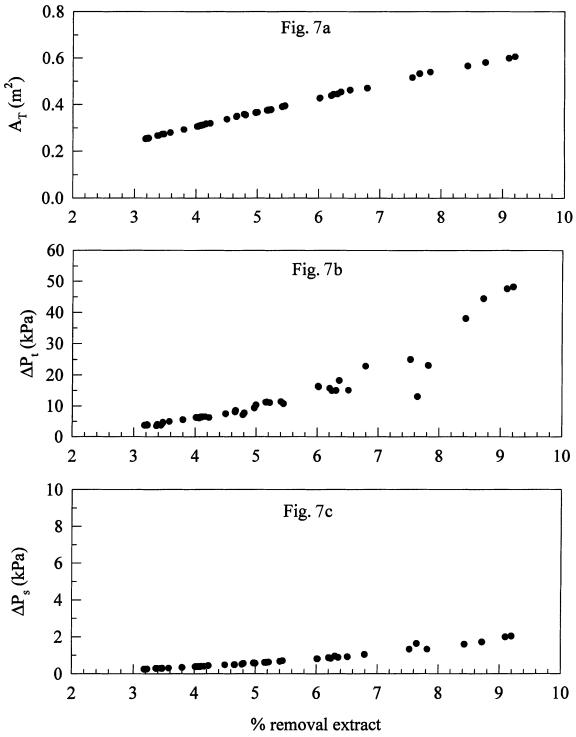

Fig. 7. Values of total membrane area required, and tube and shell side pressure drops for the different points on the Pareto set of Fig. 5a.

r_i is associated with much larger increases in the rates of mass transfer, and therefore much larger increases in both R_a and R_e, than is possible with changes in Q_s. The much lower slope of the Pareto set in Fig. 4a as compared to that in Fig. 5a, further confirms this point. This sensitivity is manifested as a dominating effect of r_i on the optimal solutions (later in this paper, we will *again* observe that the Pareto optimal solutions are quite insensitive to changes in the values of Q_s).

A considerable amount of physical insight is gained by solving *several* simpler optimization problems involving smaller amounts of freedom, for example, problems with only one or two decision variables. For the multi-objective optimization of membrane modules, we solved four such problems involving two decision variables each. In all these simplified problems, one of the decision variables was selected as Q_s. The values of three of the other design variables (in Eqs. (3a) and (3b)) were kept fixed at reference values while the remaining one (by turns) was allowed to vary. It was found that in *all* these problems, the optimal value of Q_s was at its upper bound of $10^{-5}\,m^3/s$. This means that the other decision variable used (r_i, l, φ or t) controls R_a and R_e in these problems. Increasing removals of alcohol and extract are associated with higher membrane areas in all four cases, and this was achieved with increasing values of l, or decreasing values of r_i, φ, or t. It should be pointed out that lower values of r_i lead to a *significant* increase in the pressure drop on the tube side, consistent with the Hagen–Poiseuille law [26,27]. An important conclusion is that changes in the physical dimensions of the module (except t) can produce a wider range of points on the Pareto set than what is possible by adjusting just the flow rate of water.

3.2.1. Sensitivity of the Pareto set to (constant) values of Q_s, l, φ and t

As discussed in the previous section, the internal radius of the hollow fiber, r_i, is the most important decision variable which controls the optimal solution. It is, therefore, natural to use r_i as the *sole* decision variable, and fix the others (Q_s, l, φ and t) at constant values. This would lead to less cumbersome design procedures. This is precisely what has been done in Problem no. 2 (Table 4), in which Q_s, l, φ and t have been kept constant. The Pareto set obtained is almost identical to that for Problem no. 1, which is not surprising, since the constant values of Q_s, l, φ and t were taken to be almost the same as those obtained in Problem no. 1. Problem no. 2 is being called as the reference (ref) case.

A sensitivity study is now carried out. The values of Q_s, l, φ and t are changed *one at a time*, and optimal solutions (with r_i as the sole decision variable) obtained. Table 4 shows details of the several (Problems nos. 3–10) studied, and Figs. 8 and 9 show the results graphically. These diagrams are useful to an engineer designing a beer dialysis module and will enable him, after targeting a particular removal percentage, to select feasible (and optimal) designs. These diagrams quantify the trade-offs available. Fig. 9 allows one to know the kind of trade-offs that can be made between r_i and one of the other four decision variables, Q_s, l, φ and t. This is useful for the case when an engineer does not want to make more than two alterations to an operational dialysis unit, as for example, if an engi-

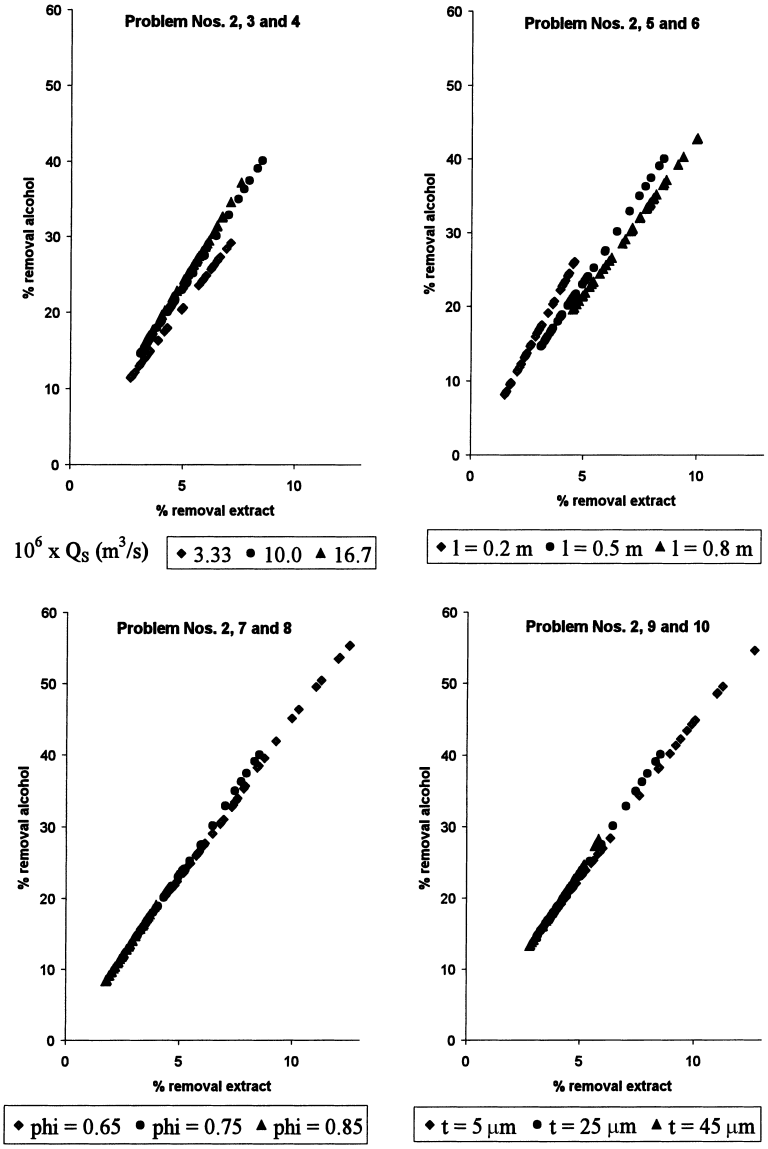

Fig. 8. Effect of Q_s, l, φ and t on the Pareto sets. r_i is the *only* decision variables used.

neer receives a new bundle of hollow fibers (to replace the old bundle which is fouled) with a larger internal radius. From the top-left chart of Fig. 8, he would find out that he has to increase the water flow rate to achieve the previous removal performance characteristic, R_a and R_e. We have also generated results for ΔP_t, ΔP_s, and A_T for the cases presented in Figs. 8 and 9, but these are not provided here for reasons of brevity (they can be supplied on request). These can be used by a designer to compute the capital costs (associated with total membrane area and other physical dimensions) and running costs (e.g. pumping costs) of the dialysis unit. It is interesting to observe from Figs. 8 and 9, Problem nos. 2–4, that the optimal solutions are quite insensitive to variations in Q_s, as mentioned earlier.

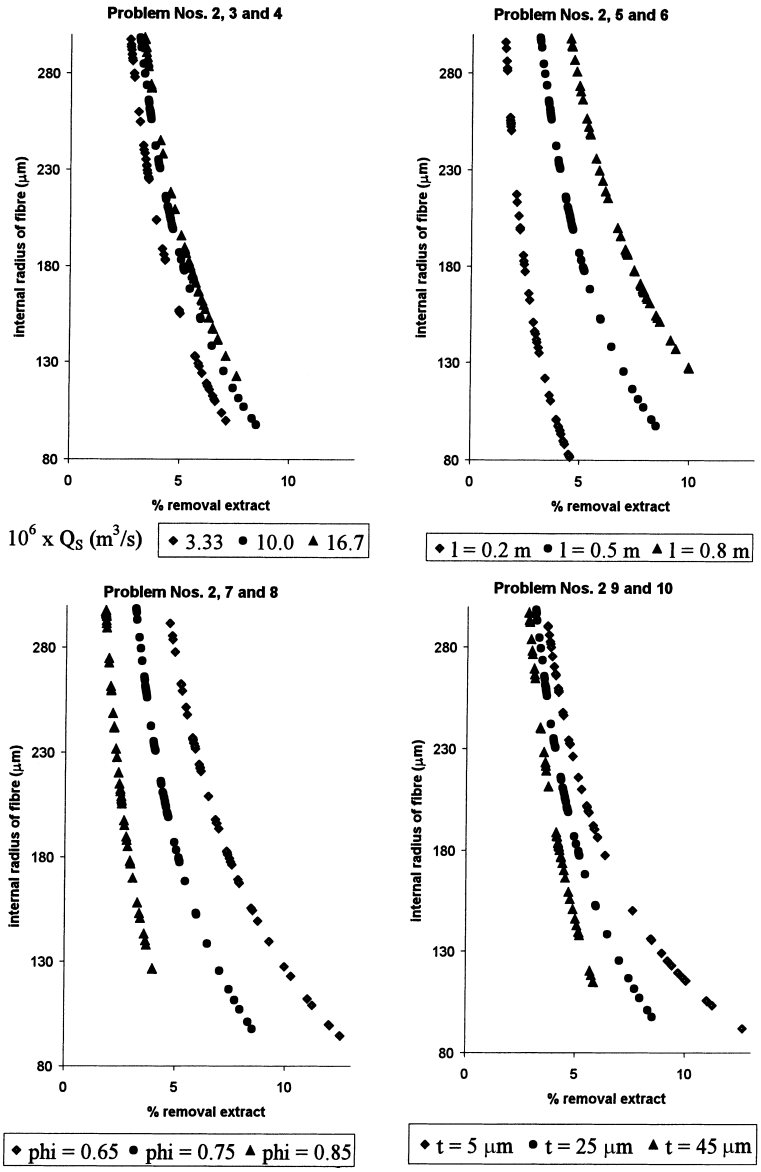

Fig. 9. Effect of Q_s, l, φ and t on the optimal value of r_i corresponding to the Paretos in Fig. 8.

3.2.2. Effects of varying the computational parameters used in NSGA

One of the important inferences obtained from the several studies discussed in the earlier sections is that the optimization process is quite sensitive to the bounds of the decision variables and the additional constraints (e.g. on ΔP_t, ΔP_s, and d_s) used. Further, it has been reported [8] that NSGA is *highly* sensitive to the values of several computational parameters used. Unfortunately, the choice of 'best' values to be used for these parameters is problem-specific, and it is difficult to know, a priori, the optimal values of the parameters to be used. We selected Problem no. 1 (Table 4) to study the effects of varying the computational parameters around the values given in Table 3. The values given in Tables 2 and 3 were kept

unchanged during this study. It was found that N_{gen}, p_{cross} and p_{mute} were the most important parameters. It was observed that as N_{gen} increased from the initial value of 0 to the final selected value of 400, the population of solutions converged to the final Pareto set shown in Fig. 5a. It is interesting to note that though the Pareto set did not show too much scatter even for N_{gen} of above about 5, this was not true of the two important decision variables, r_i and Q_s. Even at N_{gen} of about 50 we found a considerable amount of scatter in the plots for these variables against R_e. It is clear that the value of N_{maxgen} should be large enough to ensure that the scatter is removed not only in the Pareto set, but *also* in the plots of the decision variables. The effect of varying p_{cross} from 0.6 to 1.0 was then studied. Increasing p_{cross}, above the reference value of 0.8, did not have much effect. However, when p_{cross} was decreased to 0.6, the performance of GA was poorer (especially in the plot of the decision variable, r_i) as the points did not spread themselves well over the optimal region. When p_{mute} was taken as 0 (local searches around points were not performed, i.e. diversity is not encouraged), there was a slight clustering effect of the points. On the other hand, when p_{mute} was increased to 0.1, the population (specially the plot of the decision variable, r_i) showed a considerable amount of scatter. It was observed that the results were quite sensitive to the value of p_{mute}. The reference value of p_{mute}=0.0001 gave us reasonable results. The actual plots are not being provided for the sake of brevity and can be supplied on request.

3.2.3. Effect of constraints

It is clear that one has to carry out an extensive amount of exploratory work before meaningful results can be obtained in any real-life problem involving multi-objective function optimization and constraints. Pressure drop constraints on both the shell and tube sides, as well as the constraint of a fixed value of d_s, are used in the optimization studies carried out (Eq. (3e), Problem no. 1). The effects of relaxing these constraints on the optimal solution are now studied.

3.2.3.1. Pressure drop constraints. Using Problem no. 1 as a reference again, two additional problems, Problem nos. 11 and 12 (see Table 4), are studied to see the effects of varying the pressure drop constraints. In Problem no. 11, the maximum allowable values of

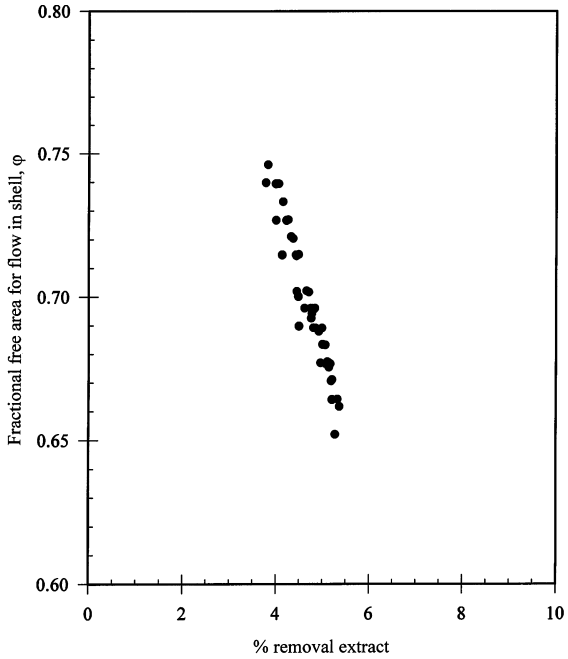

Fig. 10. Variation of the fractional free area, φ, for Problem no. 12.

ΔP_t and ΔP_s are taken at very high values, which is equivalent to removing these from Eqs. (3c) and (3d). It was found that use of none or very high upper bounds on the pressure drops (on both the shell and tube sides), leads to optimal solutions which are *almost* identical to those shown in Figs. 5 and 6 but higher values of R_e are attained. This is expected since Fig. 7b shows that the constraint on ΔP_t was not allowing this to happen in Problem no. 1 and r_i was not going down to its lower bound of 80 μm in that problem (as it does now). When the pressure drop constraints are set very low, as in Problem no. 12, the domain of R_e is *quite* small (even though the points on the Pareto set superpose on those in Fig. 5a). Interestingly, the fractional free area, φ, varies with R_e (see Fig. 10), while r_i remains almost constant at about 255 μm. This is to be expected intuitively, as the upper bound on ΔP_t does not permit a decrease in r_i, and φ decreases to accommodate more membrane area to give higher R_e.

3.2.3.2. Effect of removing the constraint on d_s. An important constraint used in Eq. (3e) is the use of a constant value for the inner diameter, d_s, of the shell (for a given flow rate of the beer). A different problem

on multi-objective optimization is now solved (Problem no. 13) in which this constraint is removed completely, but an additional decision variable, the total membrane area, A_T, is incorporated. Problem no. 13 is, thus, described by

$$\min f_1(Q_s, r_i, l, \varphi, t, A_T) = R_e \quad (5a)$$

$$\min f_2(Q_s, r_i, l, \varphi, t, A_T) = \frac{1}{1 + R_a} \quad (5b)$$

s.t.

$$0 \leq \Delta P_t \leq 51.7\,\text{kPa (7.5 psi)} \quad (5c)$$

$$0 \leq \Delta P_s \leq 10.3\,\text{kPa (1.5 psi)} \quad (5d)$$

model equations (Appendix A) (5e)

Table 4 provides the various bounds on this problem. It is clear that the use of A_T along with r_i, l, φ and t implies that the number of fibers, N, in the membrane module is being used as an additional decision variable during optimization. In Problem no. 1, the use of a fixed value of d_{shell}, with optimal values of r_i, φ and t, automatically determined the value of N to be used, while the total membrane area was computed from the optimal values of r_i, φ and t, as well as l.

Fig. 11 shows the results obtained for this problem. It is found that A_T (or N) is the *only* decision variable that varies for this case, and that all the remaining variables, namely, Q_s, r_i, l, φ and t, are found to be (almost) constant ($Q_s = 1\times10^{-5}\,m^3/s$, $r_i = 194.7\,\mu m$, $l = 0.598\,m$, $\varphi = 0.66$ and $t = 11.6\,\mu m$) under optimal conditions. It is interesting to note that the Pareto set covers a smaller domain. This is due to the upper bound used for A_T. The values of ΔP_t and ΔP_s are found to decrease as R_a and R_e increase (plots not provided), in contrast to their behavior in the earlier problems. This is because the optimal design is achieved in this problem by the use of higher values of N (or A_T), while keeping r_i, l, φ and t constant.

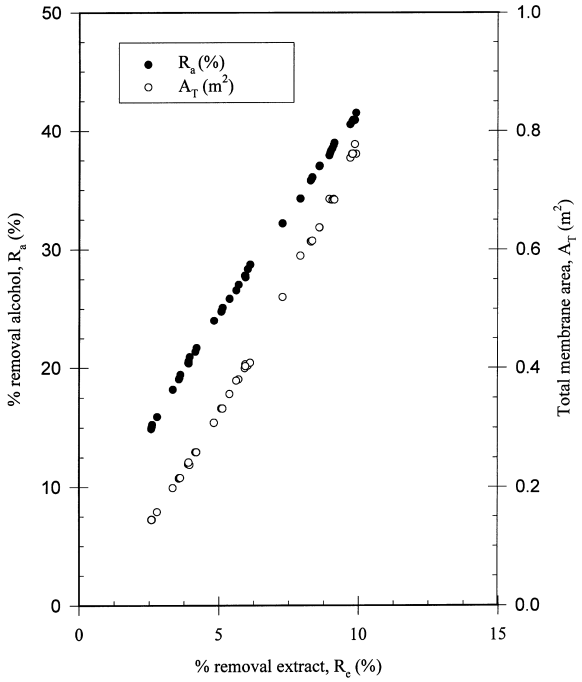

Fig. 11. Pareto set and A_T for Problem no. 13.

3.3. Cost optimization of a beer dialysis module

As mentioned earlier, a multitude of multi-objective optimization problems can be formulated, some involving even more than the two objective functions studied till now. Our aim was to provide a few simple illustrative examples only (Eqs. (3a)–(3f) and Eqs. (5a)–(5e)), and point out how one has to solve some simpler problems to develop insights. Yet another objective function which could be added is the cost. A cost function, Costfn, consisting of two terms, one related to the annualized cost of the required membrane area, while the other related to the running cost required due to the pumping of water and alcohol through the shell and tube sides, can be defined as

$$\text{Costfn} = A_T + \kappa[(\Delta P_s)(Q_s) + (\Delta P_t)(Q_{t,i})] \quad (6)$$

In this equation, κ is an empirical cost factor, related to the relative importance of the two costs. Minimization of Costfn (for a specified κ) could be added as the third objective function in either Eqs. (3a)–(3f) or Eqs. (5a)–(5e) and solutions obtained. Pareto *surfaces* in a multi-dimensional decision variable space would then be generated.

A very interesting observation was made during our exploration of the solution of the three-objective function problem described above. We combined the ε-constraint method (which also overcomes the convexity problem) with NSGA and instead of solving the three-objective function problem we solved the fol-

lowing two-objective function problem using NSGA:

$$\min f_1(Q_s, r_i, l, \varphi, t) = R_e \quad (7a)$$

$$\min f_2(Q_s, r_i, l, \varphi, t) = \text{Costfn} \quad (7b)$$

s.t.

$$R_a - \varepsilon = 0 \quad (7c)$$

$$0 \le \Delta P_t \le 51.7\,\text{kPa}\ (7.5\,\text{psi}) \quad (7d)$$

$$0 \le \Delta P_s \le 10.3\,\text{kPa}\ (1.5\,\text{psi}) \quad (7e)$$

$$d_s = 0.02103\,\text{m} \quad (7f)$$

$$\text{model equations (Appendix A)} \quad (7g)$$

In the above equations, ε is a constant (which could be varied over a suitable range to cover the entire domain of the three-dimensional objective function space). A penalty function method [8] was used, with a penalty of $10^8 \times [1-(R_a/\varepsilon)]^2$ added to both the objective functions in Eqs. (7a) and (7b) to obtain the results.

This optimization problem was solved using the same bounds of the decision variables as used in Problem no. 1 (Table 4). Interestingly, the solution of this multi-objective optimization problem for any ε, turned out to be a unique point (i.e. no Costfn versus R_e Pareto was obtained). Fig. 12 shows the results of Eqs. (7a–g) for three values of ε and with $\kappa=11$ (assumed, see later too). Table 5 lists the optimal values of the decision variables and R_e. These values of the decision variables and R_e were found to be the same for two

Table 5
Optimal values obtained for the optimization problem described by Eqs. (7a)–(7g)

Variables	Bounds	ε (%)=20	ε (%)=30	ε (%)=40
$10^6 \times Q_s$ (m^3/s)	5–10	6.21	6.38	7.66
r_i (μm)	80–300	242	177	211
l (m)	0.5–1.0	0.50	0.71	0.93
φ	0.65–0.75	0.71	0.74	0.67
t (μm)	5–25	19.6	16.6	15.4
A_T (m^2)	Calculated	0.3635	0.60	0.8884
ΔP_t (kPa)	<51.7	4.8	14.7	10.0
ΔP_s (kPa)	<10.3	0.39	0.69	1.8
Pareto points κ=1, 11, 20				
R_a (=ε) (%)		20	30	40
R_e (%)		4.54	7.25	10.18
Costfn				
κ=1		0.39	0.67	0.94
κ=11		0.61	1.32	1.50
κ=20		0.81	1.92	2.00

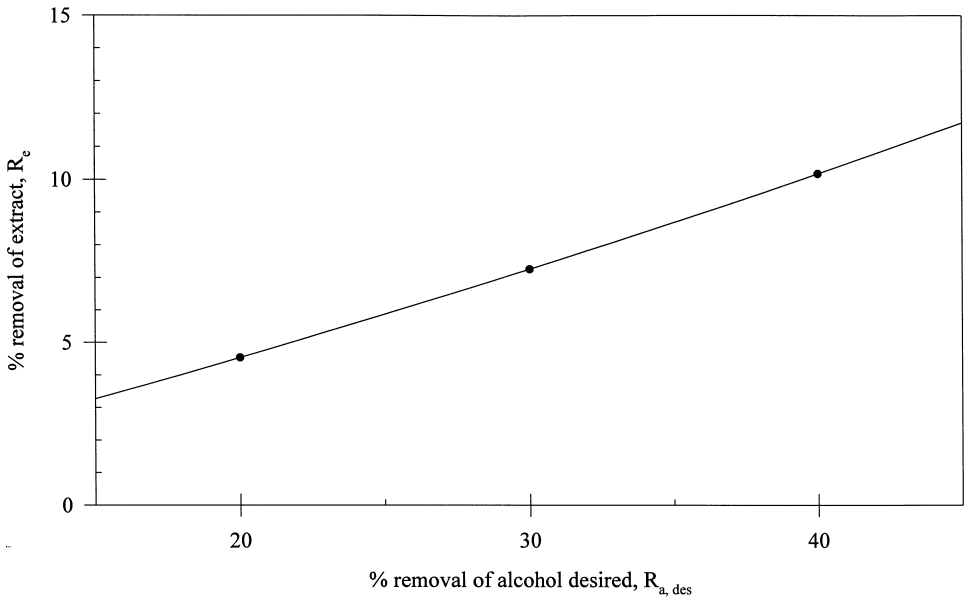

Fig. 12. Unique optimum values of R_e (%) obtained for different values of ε (=desired value, $R_{a,des}$ (%)) for the problem defined in Eqs. (7a–g).

other values of κ between 1 and 20 (though the optimal value of Costfn varied with κ as given in Table 5). The uniqueness of the solutions of Eqs. (7a–g) for different ε suggests that the Pareto *surface* in the three-dimensional Costfn-R_a-R_e space is just a *curve* (and not a three-dimensional *surface*). This curve can easily be imagined and drawn using Fig. 12. In fact, three points on this curve are given in Table 5 (for $\kappa=11$). The optimal values of the five decision variables in this three-dimensional problem, though independent of κ, are not found to be the same for different points on the Pareto set.

We also studied the effect of varying the two important model parameters, P_{ma} and z, on the optimal solutions of the reference problem. The results are not shown here for the sake of brevity again, but can be supplied on request. Such a sensitivity study can account for the inadequacies of the model (plant-model mismatch) and one could look at the diffused Pareto *zones* so generated. Variation of P_{ma} would also account for the changes in the pore size of the membrane in a problem where membrane design is also part of the total design, and we are not just studying the optimization of the design of the module alone.

4. Conclusions

In this study, we have developed a simple model for a beer dialysis module and have tuned it using some (scarce) experimental results on a laboratory-scale module [4]. The model is then used to carry out multi-objective optimization of a beer dialysis module in the presence of a few constraints. This optimization is done using a very robust, AI-based technique, NSGA. Several simple two-objective function and one three-objective function problems involving the maximization of the alcohol removal from the beer, minimization of the removal of extract and minimization of the cost, have been studied to illustrate the procedures and explain and interpret the results obtained. One needs to solve several simpler optimization problems with just one or two decision variables (smaller amount of freedom), to gain insight and to provide help in formulating the more general multi-objective optimization problem. A Pareto optimal curve is obtained for the three-objective function problem, using a mixture of the ε-constraint method and NSGA.

5. Nomenclature

A	area (m^2)
C	concentration (mol/m^3)
ΔC	concentration difference (mol/m^3)
d	diameter (m)
D	diffusion coefficient (m^2/s)
f	objective function
F	Fanning friction factor
k	mass transfer coefficient (m/s)
l	length of each fiber (m)
M	molecular weight (kg/mol)
n	number of atoms in an extract molecule
N	number of fibers in a module
p	probability
P	permeability (m/s), pitch (m)
ΔP	pressure drop (Pa)
Q	flow rate (m^3/s)
r	radius (m)
R	percentage removal (%)
Re	Reynolds number
S	rate of transfer of alcohol or extract (mol/s)
Sc	Schmidt number
Sh	Sherwood number
t	thickness (m)
T	temperature (K)
v	average velocity (m/s)
V	volume fraction (m^3/m^3 soln)
w	weighting factor
z	number of rings in an extract molecule

Greek symbols

ψ	association factor for solvent
μ	viscosity (Pa s)
ν	molar volume (m^3/mol)
ε	constant value of R_a
φ	fractional free area for flow in shell
ρ	density (kg/m^3)
κ	empirical cost weightage factor

Subscripts/superscripts

a	alcohol
C	carbon
cross	crossover
des	desired
e	extract
eq	equivalent
H	hydrogen

i	inlet, inner
lm	log mean
m	membrane
mute	mutation
o	outlet, outer
O	oxygen
ov	overall
p	t (tube) or s (shell)
q	i (inlet) or o (outlet)
r	a (alcohol) or e (extract)
t	tube
T	total
s	shell
w	water

Acknowledgements

We like to thank Dr. Li Kang of the Department of Chemical and Environmental Engineering, National University of Singapore, Singapore, whose design problem for a course-project provided the stimulus for this work. One of the authors (S.K. Gupta) gratefully acknowledges the hospitality and facilities provided to him by the Department of Chemical Engineering, University of Wisconsin, Madison, WI, USA, where this paper was revised.

Appendix A. List of equations in beer dialysis model

A.1. Mass balances

Overall and component (alcohol and extract) mass balance equations

$$Q_{t,i} + Q_s \frac{1}{1 - V_{s,ai} - V_{s,ei}} = Q_{t,o} + Q_s \frac{1}{1 - V_{s,ao} - V_{s,eo}} \quad (A.1)$$

$$Q_{t,i} V_{t,ri} + Q_s \frac{V_{s,ri}}{1 - V_{s,ai} - V_{s,ei}} = Q_{t,o} V_{t,ro} + Q_s \frac{V_{s,ro}}{1 - V_{s,ao} - V_{s,eo}} \quad (A.2)$$

$$R_r = \left(\frac{Q_{t,i} V_{t,ri} - Q_{t,o} V_{t,ro}}{Q_{t,i} V_{t,ri}} \right) \times 100 = \left(1 - \frac{Q_{t,o} V_{t,ro}}{Q_{t,i} V_{t,ri}} \right) \times 100 \quad (A.3)$$

In all the equations, subscript p, q and r takes the values as follows: p=t (tube) or s (shell), q=i (inlet) or o (outlet), r=a (alcohol) or e (extract).

The rate of transfer of a particular solute, $r=S_r=k_{ov,r}A_{T,r}\Delta C_{lm,r}$, where

$$S_r = Q_s \frac{\rho_r}{M_r} \left[\frac{V_{s,ro}}{1 - V_{s,ao} - V_{s,eo}} - \frac{V_{s,ri}}{1 - V_{s,ai} - V_{s,ei}} \right] \quad (A.4)$$

$$\Delta C_{lm,r} = \frac{(C_{t,ri} - C_{s,ro}) - (C_{t,ro} - C_{s,ri})}{\ln[(C_{t,ri} - C_{s,ro})/(C_{t,ro} - C_{s,ri})]} \quad (A.5)$$

$$C_{p,rq} = \frac{\rho_r}{M_r} V_{p,rq} \quad (A.6)$$

$$D_{aw} = \frac{7.4 \times 10^{-8} (\psi_w M_w)^{1/2} T}{\mu_w \nu_a^{0.6}} \quad (A.7)$$

$$D_{ew} = D_{aw} \left(\frac{\nu_a}{\nu_e} \right)^{0.6} \quad (A.8)$$

$$\nu_e = (n_C \times 14.8) + (n_H \times 3.7) + (n_O \times 7.4) - (z \times 15) \quad (A.9)$$

where z is the number of glucose units in a molecule of the extract (see Fig. 3), and $n_C=6\times z$, $n_H=(10\times z)+2$, and $n_O=(5\times z)+1$.

The permeability of the membrane for the alcohol and the extract was calculated using a plot of the normalized diffusivity, (D_m/D), as a function of the molecular weight of the solute, where D is the binary diffusion coefficient of any solute in water and D_m the effective solute diffusivity in the membrane [1]. The membrane permeabilities are related to the effective solute diffusivities by [1]

$$\frac{P_{mE}}{P_{mA}} = \frac{D_{mE}}{D_{mA}} \quad (A.10)$$

A.2. Physical dimensions of the membrane module

$$N = \frac{A_T}{2\pi r_i l}, \qquad r_o = r_i + t,$$
$$A_s = \frac{N(\sqrt{3}P_t^2 - 2\pi r_o^2)}{2} = \frac{N\pi r_o d_{eq}}{2} \quad (A.11)$$

$$d_s = \sqrt{\frac{2\sqrt{3}N}{\pi}} P_t, \qquad \varphi = 1 - N\left(\frac{2r_o}{d_s}\right)^2,$$
$$d_{eq} = \frac{\sqrt{3}P_t^2 - 2\pi r_o^2}{\pi r_o} \tag{A.12}$$

A.3. Shell side mass transfer

$$v_s = \frac{Q_s}{A_s}\frac{1}{1 - V_{s,ai} - V_{s,ei}}, \qquad Re_s = \frac{d_{eq}\rho_w v_s}{\mu_w},$$
$$Sc_r = \frac{\mu_w}{\rho_w D_{rw}} \tag{A.13}$$

$$Sh_{s,a} = \frac{k_{s,a}d_{eq}}{D_{aw}}, \qquad Sh_{s,e} = \frac{k_{s,e}d_{eq}}{D_{ew}} \tag{A.14}$$

$$Sh_{s,a} = \begin{cases} 0.025 \times (Re_s^{0.94}\, Sc_a^{0.33}), & \text{for } Re_s > 2100, \\ 1.62 \times \left(Re_s\, Sc_a \dfrac{d_{eq}}{l}\right)^{0.33}, & \text{for } Re_s \le 2100 \end{cases} \tag{A.15}$$

$$\text{If } Sh_{s,a} < 4.0, \quad Sh_{s,a} = 4.0 \tag{A.16}$$

$$Sh_{s,e} = \begin{cases} 0.025 \times (Re_s^{0.94} Sc_e^{0.33}), & \text{for } Re_s > 2100, \\ 1.62 \times \left(Re_s Sc_e \dfrac{d_{eq}}{l}\right)^{0.33}, & \text{for } Re_s \le 2100 \end{cases} \tag{A.17}$$

$$\text{If } Sh_{s,e} < 4.0, \quad Sh_{s,e} = 4.0 \tag{A.18}$$

A.4. Tube side mass transfer

$$v_t = \frac{Q_{t,o}}{\pi N r_i^2}, \qquad Re_t = \frac{2r_i\rho_w v_t}{\mu_w},$$
$$Sh_{t,a} = \frac{k_{t,a}(2r_i)}{D_{aw}}, \qquad Sh_{t,e} = \frac{k_{t,e}(2r_i)}{D_{ew}} \tag{A.19}$$

$$Sh_{t,a} = \begin{cases} 0.025 \times (Re_t^{0.94} Sc_a^{0.33}), & \text{for } Re_t > 2100, \\ 1.62 \times \left(Re_t Sc_a \dfrac{2r_i}{l}\right)^{0.33}, & \text{for } Re_t \le 2100 \end{cases} \tag{A.20}$$

$$\text{if } Sh_{t,a} < 4.0 \quad Sh_{t,a} = 4.0 \tag{A.21}$$

$$Sh_{t,e} = \begin{cases} 0.025 \times (Re_t^{0.94} Sc_e^{0.33}), & \text{for } Re_t > 2100, \\ 1.62 \times \left(Re_t Sc_e \dfrac{2r_i}{l}\right)^{0.33}, & \text{for } Re_t \le 2100 \end{cases}$$

$$\text{if } Sh_{t,e} < 4.0 \quad Sh_{t,e} = 4.0 \tag{A.22}$$

A.5. Overall

$$\frac{1}{k_{ov,r}} = \frac{1}{k_{t,r}} + \frac{1}{P_{m,r}} + \frac{1}{k_{s,r}} \tag{A.23}$$

A.6. Shell side pressure drop equations

$$\Delta P_s = \frac{2F_s l v_s^2 \rho_w}{d_{eq}} \tag{A.24}$$

$$F_s = \begin{cases} 0.0014 + \left(\dfrac{0.125}{Re_s^{0.32}}\right), & \text{for } Re_s > 2100, \\ \dfrac{16}{Re_s}, & \text{for } Re_s \le 2100 \end{cases} \tag{A.25}$$

A.7. Tube side pressure drop equations

$$\Delta P_t = \frac{F_t l v_t^2 \rho_w}{r_i} \tag{A.26}$$

$$F_t = \begin{cases} 0.0014 + \left(\dfrac{0.125}{Re_t^{0.32}}\right), & \text{for } Re_t > 2100, \\ \dfrac{16}{Re_t}, & \text{for } Re_t \le 2100 \end{cases} \tag{A.27}$$

References

[1] W.S.W. Ho, K.K. Sirkar (Eds.), Membrane Handbook, Van Nostrand Reinhold, New York, 1992.

[2] H. Moonen, H.J. Niefind, Alcohol reduction in beer by means of dialysis, Desalination 41 (1982) 327.

[3] I. Leskosek, M. Mitrovic, Optimization of beer dialysis with cuprophane membranes, J. Ins. Brewing 100 (1994) 287.

[4] I. Leskosek, M. Mitrovic, V. Nedovic, Factors influencing alcohol and extract separation in beer dialysis, World J. Microbiol. Biotechnol. 11 (1995) 512.

[5] I. Leskosek, M. Mitrovic, V. Nedovic, Influence of beer flow rate on mass transfer kinetics in beer Dialysis, Biotechnol. Tech. 2 (1993) 123.
[6] J.H. Holland, Adaptation in Natural and Artificial Systems: An Introductory Analysis with Applications to Biology, Control and Artificial Intelligence, University of Michigan Press, Ann Arbor, 1975.
[7] D.E. Goldberg, Genetic Algorithms in Search, Optimization, and Machine Learning, Addison-Wesley, Reading, MA., 1989.
[8] K. Deb, Optimization for Engineering Design: Algorithms and Examples, Prentice Hall, New Delhi, India, 1995.
[9] K. Deb, Evolutionary algorithms for multi-criterion optimization in engineering design, in: K. Miettinen, P. Neittaanmäki, M.M. Mäkelä, J. Périaux (Eds.), Evolutionary Algorithms in Engineering and Computer Science: Recent Advances in Genetic Algorithms, Evolution Strategies, Evolutionary Programming, Genetic Programming and Industrial Applications, Wiley, New York, 1999.
[10] C.M. Fonseca, P.J. Fleming, Multiobjective optimization and multiple constraint handling with evolutionary algorithms, Part I: A unified formulation, IEEE Trans. Syst. Man. Cy. A28 (1998) 26.
[11] A. Goicoechea, D.R. Hansen, L. Duckstein, Multiobjective Decision Analysis with Engineering and Business Applications, Wiley, New York, 1982.
[12] V. Chankong, Y.Y. Haimes, Multiobjective Decision Making — Theory and Methodology, Elsevier, New York, 1983.
[13] Y.Y. Haimes, Hierarchical Analysis of Water Resources Systems: Modeling and Optimization of Large-Scale Systems, McGraw-Hill, New York, 1977.
[14] S.H. Hollingdale, in: J. Lighthill (Ed.), Methods of Operational Analysis in Newer Uses of Mathematics, Penguin, New York, 1978.
[15] P.J. Fleming, Applications of multiobjective optimization to compensator design for SISO control systems, Electron. Lett. 22 (1986) 258.
[16] P.J. Fleming, Computer-aided control system design of regulators using a multiobjective optimization approach, in: Proceedings of IFAC Control Applications of Nonlinear Program and Optimization, Capri, Italy, 1985, pp. 47–52.
[17] N. Srinivas, K. Deb, Multiobjective optimization using nondominated sorting in genetic algorithms, Evol. Comput. 2 (1995) 106.
[18] K. Mitra, K. Deb, S.K. Gupta, Multiobjective dynamic optimization of an industrial nylon 6 semibatch reactor using genetic algorithm, J. Appl. Polym. Sci. 69 (1998) 69.
[19] R.R. Gupta, S.K. Gupta, Multiobjective optimization of an industrial nylon-6 semibatch reactor system using genetic algorithm, J. Appl. Polym. Sci. 73 (1999) 729.
[20] V. Bhaskar, S.K. Gupta, A.K. Ray, Multiobjective optimization of an industrial wiped film poly(ethylene terephthalate) reactor, AIChE J. 46 (5) (2000) 1046.
[21] J.K. Rajesh, S.K. Gupta, G.P. Rangaiah, A.K. Ray, Multiobjective optimization of steam reformer performance using genetic algorithm, Ind. Eng. Chem. Res. 39 (3) (2000) 706.
[22] G. Ravi, S.K. Gupta, M.B. Ray, Multiobjective optimization of cyclone separators, Ind. Eng. Chem. Res., (2000), in press.
[23] V. Bhaskar, S.K. Gupta, A.K. Ray, Applications of multiobjective optimization in chemical engineering, Rev. Chem. Eng. 16 (1) (2000) 1.
[24] R.H. Perry, D.W. Green, J.O. Maloney (Eds.), Perry's Chemical Engineers' Handbook, 7th Edition, McGraw-Hill, New York, 1997.
[25] J.D. Seader, E.J. Henley, Separation Process Principles, Wiley, New York, 1997.
[26] W.L. McCabe, J.C. Smith, P. Harriott, Unit Operations of Chemical Engineering, 5th Edition, McGraw-Hill, New York, 1993.
[27] V. Gupta, S. K. Gupta, Fluid Mechanics and its Applications, New Age Intl., New Delhi, India, 1984.